

# Impact of Mode Dispersion on Cross-Phase Modulation in Few-Mode Fiber Transmissions

C. Lasagni<sup>(1)</sup>, P. Serena<sup>(1)</sup>, A. Bononi<sup>(1)</sup>, A. Mecozzi<sup>(2)</sup>, C. Antonelli<sup>(2)</sup>

<sup>(1)</sup>Università di Parma, Dip. Ingegneria e Architettura, 43124 Parma (Italy) ✉ chiara.lasagni@unipr.it

<sup>(2)</sup>Università dell'Aquila, Dip. Scienze Fisiche e Chimiche, 67100 L'Aquila (Italy)

**Abstract** We show that random mode dispersion within groups of quasi-degenerate modes in few-mode fibers considerably affects the dependence of the cross-phase modulation variance on the systematic differential delay between mode groups. We present a perturbative model that accounts for the two propagation effects. ©2023 The Authors

## Introduction

Space-division multiplexed (SDM) systems based on few-mode fibers (FMFs) support the propagation of groups of quasi-degenerate modes. While modes in the same group are completely entangled due to strong linear coupling, the linear crosstalk between different groups is typically small<sup>[1]</sup>. However, the groups interact nonlinearly while propagating along the optical fiber<sup>[2]–[5]</sup>. The strength of such interaction depends, among other aspects, on the differential mode group delay (DMGD) between the groups and the spatial mode dispersion (SMD) within each mode group.

Due to the complexity of SDM systems, simple perturbative models are the only practical analytical approach to study these nonlinear effects. In<sup>[6]–[10]</sup> the authors showed that the change of channel walk-off caused by DMGD alters the four-wave mixing (FWM) efficiency, causing nonlinear resonances for novel frequency configurations. The authors in<sup>[9]</sup> proposed an SDM extension of the Gaussian noise (GN) model<sup>[11]</sup> accounting for DMGD but neglecting SMD. In<sup>[12]</sup>, the nonlinear interference noise (NLIN) model<sup>[13]</sup> was generalized to SDM, including the impact of SMD in the cross-phase modulation (XPM) variance by assuming large SMD values and neglecting the effect of SMD within a channel bandwidth. Recently, the ergodic GN model has been proposed in<sup>[14]</sup> to account for arbitrary values of SMD on the XPM variance, showing a significant impact in strong coupling conditions. However, none of these models investigated the joint effects of DMGD and SMD in the regime of weak-coupling.

In this work, we fill this gap by extending the work in<sup>[14]</sup> to the case of FMFs in the presence of DMGD and SMD. We show that SMD plays an important role in mitigating the XPM resonance induced by DMGD, and we propose an approximated formula for its estimation.

## Perturbative model

We consider an FMF supporting two groups of quasi-degenerate modes labeled as  $a$  and  $b$ , with  $2N_a$  and  $2N_b$  polarization modes, respectively. We express the transmitted signal in group  $s$  as:

$$|E_s(t)\rangle = \sum_{\mathbf{n}} s_{\mathbf{n}} |G_{\mathbf{n}}(t)\rangle, \quad s \in (a, b) \quad (1)$$

where the symbol  $|\cdot\rangle$  indicates a  $2N_s$  column vector and  $\sum_{\mathbf{n}}$  is a short-hand notation for a triple summation over  $\mathbf{n} = (n_1, n_2, n_3)$ . The index triplet represents a channel access such that  $s_{\mathbf{n}}$  is a transmitted symbol at time lag  $n_1$ , frequency channel index  $n_2$ , and polarization mode  $n_3$  in group  $s$ . The vector  $|G_{\mathbf{n}}(t)\rangle \triangleq p(t - n_1 T) e^{j\Omega_{n_2} t} |n_3\rangle$  is the shaping function with  $p$  the supporting pulse,  $T$  the symbol time,  $\Omega_{n_2}$  the carrier frequency, and  $|n_3\rangle$  a standard unit vector identifying the carrier polarization in group  $s$ .

For  $N_a=1$  and  $N_b=2$ , the linear mode coupling along distance is sketched in Fig. 1(left), where dashed/solid lines indicate weak/strong coupling. Figure 1(center) depicts a pulse in each polarization at a given propagation distance. The DMGD causes a systematic delay among the pulses in the two groups due to different group velocities, while the SMD yields a random delay in a group.

Within a perturbative approximation of the coupled Manakov equations with multiple groups<sup>[3]</sup>, the NLIN on the transmitted symbol  $a_i$  can be modeled as the following additive noise:

$$n_i = -j \sum_{\mathbf{h}, \mathbf{l}, \mathbf{n}} \underbrace{a_{\mathbf{h}}^* a_{\mathbf{l}} a_{\mathbf{n}} \mathcal{X}_{\mathbf{h}\mathbf{l}\mathbf{n}i}}_{\text{intra-group}} - j \sum_{\mathbf{k}, \mathbf{m}, \mathbf{n}} \underbrace{b_{\mathbf{k}}^* b_{\mathbf{m}} a_{\mathbf{n}} \mathcal{X}'_{\mathbf{k}\mathbf{m}\mathbf{n}i}}_{\text{inter-group}} \quad (2)$$

where  $\mathcal{X}_{\mathbf{h}\mathbf{l}\mathbf{n}i}$  and  $\mathcal{X}'_{\mathbf{k}\mathbf{m}\mathbf{n}i}$  express the intra- and inter-group FWM combinations, respectively. The intra-group FWM was modeled in<sup>[14]</sup> accounting for the distance- and frequency-dependent polarization mixing induced by SMD on the FWM efficiency. Here we extend the theory to the inter-group term accounting for DMGD and SMD. Ne-

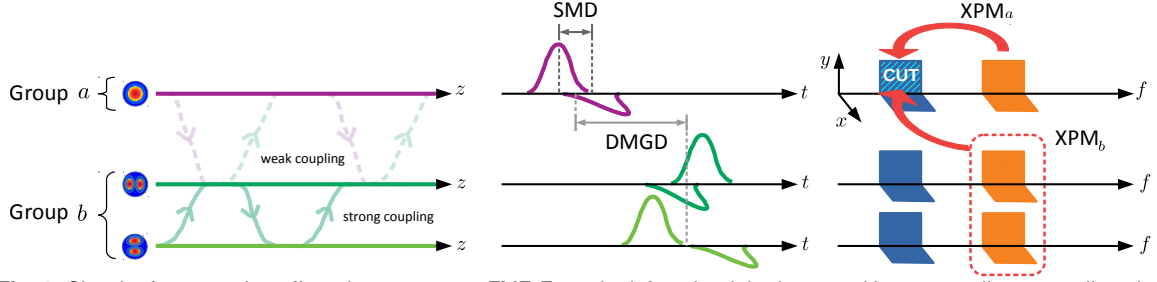


**Fig. 1:** Sketch of propagation effects in a two-group FMF. From the left to the right: intra- and inter-group linear coupling along propagation distance; random delay induced by SMD between polarization modes within a group of quasi-degenerate modes and deterministic DMGD between the centers of mass of the two groups; intra- and inter-group XPM on the channel under test.

glecting the inter-group linear coupling, we find that the FWM between frequencies  $\{\omega_j\}_{j=1}^4$  is weighted by the following link kernel,

$$\eta_{\mathbf{k}\mathbf{m}\mathbf{n}\mathbf{i}} = \int_0^{L_t} f(z) e^{-j\Delta\beta z} P_{k_3 m_3}^{(b)}(z) Q_{i_3 n_3}^{(a)}(z) dz \quad (3)$$

where  $L_t$  is the total link length,  $f(z)$  is the power loss/gain at coordinate  $z$ , and  $\Delta\beta$  is the phase-matching coefficient between the interacting frequencies  $\omega_j$ , including the extra walk-off induced by the DMGD<sup>[6],[8]</sup>. The matrices  $\mathbf{Q}^{(a)} = [Q_{ij}^{(a)}]$  and  $\mathbf{P}^{(b)} = [P_{ij}^{(b)}]$  are defined as  $\mathbf{Q}^{(a)} \triangleq \mathbf{U}_a^\dagger(z, \omega_1) \mathbf{U}_a(z, \omega_2)$  and  $\mathbf{P}^{(b)} \triangleq \mathbf{U}_b^\dagger(z, \omega_3) \mathbf{U}_b(z, \omega_4)$ , with  $\dagger$  the transpose-conjugate, and  $\mathbf{U}_{a,b}$  independent unitary matrices accounting for frequency-dependent random mode coupling within group  $(a, b)$ .

We now concentrate on XPM. Since, under perturbative assumptions, XPM is additive in the number of channels<sup>[11]</sup>, we focus on two frequency channels. Figure 1(right) defines the XPM on the channel under test (CUT), i.e., a polarization of a frequency channel in group  $a$ , due to channels in groups  $a$  ( $\text{XPM}_a$ ) and  $b$  ( $\text{XPM}_b$ ).

## Results

Due to the randomness of the mode coupling process, the link kernel in (3), and thus the XPM and its variance, are random variables. Following the idea of the ergodic GN model<sup>[14]</sup>, we focus on the average value of the XPM variance with respect to the random mode coupling process. Since for Gaussian distributed symbols the XPM variance depends on  $|\eta_{\mathbf{k}\mathbf{m}\mathbf{n}\mathbf{i}}|^2$ , its average involves the expectation of the product of four random matrices in each group. We evaluated such expectation obtaining a semi-analytical model for the average  $\text{XPM}_b$  variance, which requires numerical integration of frequency integrals over the  $\omega_j$ . Summing such result to the  $\text{XPM}_a$  variance given in<sup>[14]</sup>, we obtain an estimation of the average XPM variance which we refer to as the *complete model*.

The analysis simplifies considerably within the

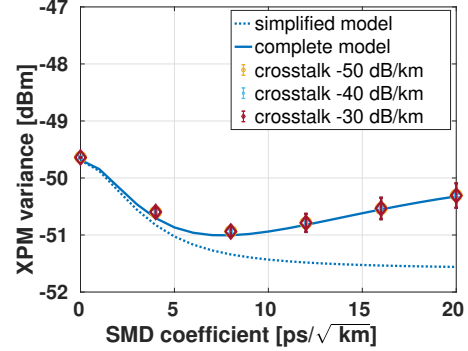


**Fig. 2:** Single-span CUT XPM variance vs SMD coefficient. Markers: SSFM for variable amount of linear group crosstalk. Solid: complete model. Dotted: simplified model by Monte Carlo integration. DMGD=0 ps/km.

inter-channel SMD approximation, which neglects the frequency dependence of SMD within a channel bandwidth<sup>[12],[14]</sup>. We obtain the following expected value,

$$\mathbb{E} [|\eta_{\mathbf{k}\mathbf{m}\mathbf{n}\mathbf{i}}|^2] = 2N_b \frac{\alpha'(\Delta\omega)}{\alpha} |\eta_0(\alpha'(\Delta\omega))|^2 \quad (4)$$

where  $\eta_0$  is the single-mode link kernel in the absence of mode dispersion<sup>[11]</sup>,  $\Delta\omega$  is the spacing between frequency channels,  $\alpha$  is the fiber attenuation, and  $\alpha'$  is an equivalent attenuation defined as  $\alpha'(\Delta\omega) \triangleq \alpha + \Delta\omega^2 (\xi_a^2 + \xi_b^2)$  with  $\xi_s^2 \triangleq \frac{\eta_{\text{SMD},s}^2}{2} \frac{N_s^2}{4N_s^2 - 1}$ ,  $s \in (a, b)$ , where  $\eta_{\text{SMD},s}$  is the SMD coefficient (typically expressed in ps/ $\sqrt{\text{km}}$ )<sup>[14],[15]</sup> in group  $s$ . Thanks to this result, we derive the following new expression for the average variance of the inter-group XPM ( $\text{XPM}_b$  in Fig. 1),

$$\mathbb{E} [\sigma_{\text{XPM},b}^2] = 2N_b \left[ \sigma_1^2(\alpha) + \frac{\alpha'}{\alpha} \sigma_1^2(\alpha'(\Delta\omega)) \right] \quad (5)$$

where  $\sigma_1^2(\alpha)$  is the single-mode XPM variance evaluated in the absence of SMD but including the DMGD (typically expressed in ps/km) in the channel walk-off.  $\sigma_1^2$  can be evaluated by numerical quadrature, such as Monte Carlo integration<sup>[16]</sup>, or by means of approximated formulas, for instance through the expressions in<sup>[14]</sup> based on the results of<sup>[11]</sup>. Here, we refer to the average XPM variance relying on the inter-channel SMD approximation for both the intra- and inter-group

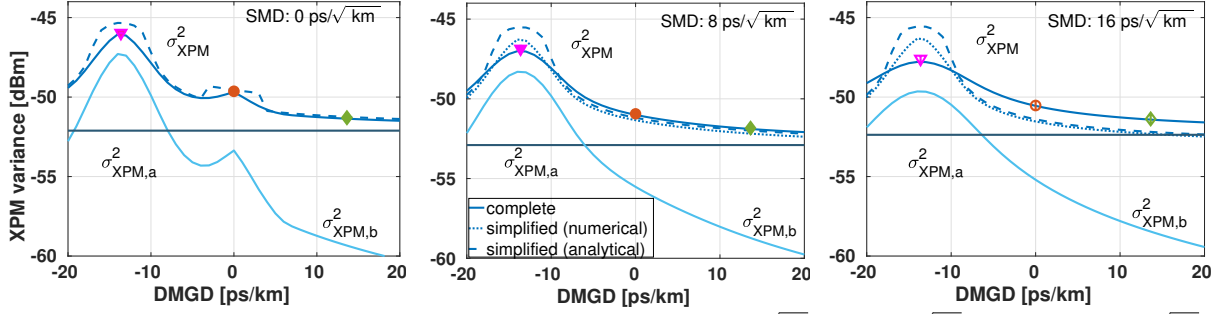


**Fig. 3:** Single-span CUT XPM variance vs DMGD, with SMD coefficient: 0 ps/√km (left), 8 ps/√km (center), and 16 ps/√km (right). Markers: SSFM results with linear crosstalk -50 dB/km. Solid lines: complete model (total XPM with its  $\sigma_{\text{XPM},a}^2$  and  $\sigma_{\text{XPM},b}^2$  contributions). Dotted lines: simplified model (numerical integration). Dashed lines: simplified model's analytical approximation.

contribution as *simplified model*.

To test the proposed models, we performed split-step Fourier method (SSFM) simulations based on a waveplate model of linear coupling with the number of waveplates and the SSFM steps set according to<sup>[17]</sup>. Since the XPM variance scales almost linearly with the number of spans<sup>[11]</sup>, we focused just on a single-span link of 100 km of FMF supporting three spatial modes in two groups, as sketched in Fig. 1, with attenuation 0.2 dB/km and chromatic dispersion 17 ps/(nm·km), both mode-independent. We computed the Manakov coefficients and the fiber nonlinearity coefficient as per Eqs. (61)–(62) in<sup>[3]</sup> with effective area 125  $\mu\text{m}^2$  for group *a*, 165  $\mu\text{m}^2$  for group *b*, and 250  $\mu\text{m}^2$  as cross-group effective area<sup>[4]</sup>. In each mode we transmitted two dual-polarization frequency channels spaced by 100 GHz, modulated with sequences of 131072 complex Gaussian distributed symbols at 49 Gbaud.

We started by investigating the effect of SMD on the XPM variance in the absence of DMGD. For the sake of simplicity, we used  $\eta_{\text{SMD},a} = \eta_{\text{SMD},b}$  despite the smaller size of group *a*, even though it is not necessary for the model. The results are shown in Fig. 2, where the markers with worst-case error bars represent the SSFM results for 100 different random realizations of the fiber waveplates, with inter-group crosstalk values equal to -50 dB/km, -40 dB/km, or -30 dB/km. It can be seen that these crosstalk levels do not affect significantly the XPM variance, thus justifying the model's assumption of no linear coupling between mode groups. As in the case of strong mode coupling among all modes studied in<sup>[14]</sup>, we observe small random deviations and the presence of a local minimum in the XPM variance around 8 ps/√km. Figure 2 shows that the prediction of the complete model (solid lines) is in excellent agreement with SSFM results and that the numerical simplified model (dotted lines) is re-

liable for moderate values of SMD. Comparable accuracy was observed even in extra simulations with more spans that are not reported in this work.

We then investigated the joint impact of DMGD and SMD on XPM. Figure 3 shows the XPM variance as a function of the DMGD for three values of the SMD coefficient. The SSFM simulations (markers) were performed at a linear crosstalk level of -50 dB/km. The figure shows a peak in the XPM variance when the DMGD (-13.6 ps/km) counterbalances the chromatic dispersion walk-off, thus enhancing the nonlinear interaction<sup>[4],[10]</sup>. However, SMD reduces the resonance in the XPM variance by restoring a walk-off between polarization modes. In this region, simulations (triangular markers) show a reduction of the XPM variance of approximately 2 dB as the SMD coefficient is increased from 0 to 16 ps/√km. The resonance in Fig. 3(left) at DMGD=0 ps/km is due to a significant cross-polarization modulation, which quickly vanishes for increasing SMD<sup>[14]</sup>.

Figure 3 also shows the contributions of  $\sigma_{\text{XPM},a}^2$  to the overall XPM variance estimated with the complete model (solid lines), confirming the relevance of  $\sigma_{\text{XPM},b}^2$  in the region of walk-off equalization by DMGD, where it exceeds  $\sigma_{\text{XPM},a}^2$  (unaltered by the DMGD). Note that the analytical approximation of the simplified model (dashed lines) is less accurate in this region, due to the inaccuracy of the scalar formulas in<sup>[11]</sup> with a small walk-off.

## Conclusions

We have shown that random mode dispersion affects the dependence of the XPM variance on the systematic mode group delay in FMF transmissions. We extended the ergodic GN model<sup>[14]</sup> to study the dependence of the XPM on mode dispersion and mode group delay in the regime of weak coupling between non-degenerate mode groups, and we proposed a simplified formula that can assist in the design of FMFs links.

## References

- [1] P. Sillard, K. Benyahya, D. Soma, G. Labroille, P. Jian, K. Igarashi, R. Ryf, N. K. Fontaine, G. Rademacher, and K. Shibahara, "Few-mode fiber technology, deployments, and systems", *Proceedings of the IEEE, JPR0C*, 2022. 3207012. DOI: 10.1109/JPR0C.2022.3207012.
- [2] S. Mumtaz, R.-J. Essiambre, and G. P. Agrawal, "Nonlinear Propagation in Multimode and Multicore Fibers: Generalization of the Manakov Equations", *J. Lightw. Technol.*, vol. 31, no. 3, pp. 398–406, 2013. DOI: 10.1109/JLT.2012.2231401.
- [3] C. Antonelli, M. Shtaif, and A. Mecozzi, "Modeling of nonlinear propagation in Space-Division Multiplexed fiber-optic transmission", *J. Lightw. Technol.*, vol. 34, no. 1, pp. 36–54, Jan. 2016. DOI: 10.1109/JLT.2015.2510511.
- [4] G. Rademacher, R. S. Luis, B. J. Puttnam, R. Maruyama, K. Aikawa, Y. Awaji, H. Furukawa, K. Petermann, and N. Wada, "Investigation of Intermodal Nonlinear Signal Distortions in Few-Mode Fiber Transmission", *J. Lightw. Technol.*, vol. 37, no. 4, pp. 1273–1279, 2019. DOI: 10.1109/JLT.2019.2892052.
- [5] F. M. Ferreira, S. Sygletos, E. Sillekens, R. Killey, A. D. Ellis, and N. J. Doran, "On the Performance of Digital Back Propagation in Spatial Multiplexing Systems", *J. Lightw. Technol.*, vol. 38, no. 10, pp. 2790–2798, 2020. DOI: 10.1109/JLT.2020.2975982.
- [6] R.-J. Essiambre, M. A. Mestre, R. Ryf, A. H. Gnauck, R. W. Tkach, A. R. Chraplyvy, Y. Sun, X. Jiang, and R. Lingle, "Experimental Investigation of Inter-Modal Four-Wave Mixing in Few-Mode Fibers", *IEEE Photonics Technology Letters*, vol. 25, no. 6, pp. 539–542, 2013. DOI: 10.1109/LPT.2013.2242881.
- [7] A. D. Ellis, N. M. Suibhne, F. C. G. Gunning, and S. Sygletos, "Expressions for the nonlinear transmission performance of multi-mode optical fiber", *Opt. Express*, vol. 21, no. 19, pp. 22834–22846, Sep. 2013. DOI: 10.1364/OE.21.022834.
- [8] Y. Xiao, R.-J. Essiambre, M. Desgroseilliers, A. M. Tulino, R. Ryf, S. Mumtaz, and G. P. Agrawal, "Theory of intermodal four-wave mixing with random linear mode coupling in few-mode fibers", *Opt. Express*, vol. 22, no. 26, pp. 32039–32059, Dec. 2014. DOI: 10.1364/OE.22.032039.
- [9] G. Rademacher and K. Petermann, "Nonlinear Gaussian Noise Model for Multimode Fibers with Space-Division Multiplexing", *J. Lightw. Technol.*, vol. 34, no. 9, pp. 2280–2287, May 2016. DOI: 10.1109/JLT.2016.2520562.
- [10] G. Rademacher, B. J. Puttnam, R. S. Luis, R. Maruyama, K. Aikawa, Y. Awaji, and H. Furukawa, "Intermodal nonlinear signal distortions in multi-span transmission with few-mode fibers", *IEEE Photonics Technology Letters*, vol. 32, no. 18, pp. 1175–1178, 2020. DOI: 10.1109/LPT.2020.3016348.
- [11] P. Poggiolini, "The GN model of non-linear propagation in uncompensated coherent optical systems", *J. Lightw. Technol.*, vol. 30, no. 24, pp. 3857–3879, Dec. 2012. DOI: 10.1109/JLT.2012.2217729.
- [12] C. Antonelli, O. Golani, M. Shtaif, and A. Mecozzi, "Nonlinear interference noise in space-division multiplexed transmission through optical fibers", *Opt. Express*, vol. 25, no. 12, pp. 13055–13078, Jun. 2017. DOI: 10.1364/OE.25.013055.
- [13] R. Dar, M. Feder, A. Mecozzi, and M. Shtaif, "Properties of nonlinear noise in long, dispersion-uncompensated fiber links", *Opt. Express*, vol. 21, no. 22, pp. 25685–25699, 2013. DOI: 10.1364/OE.21.025685.
- [14] P. Serena, C. Lasagni, A. Bononi, C. Antonelli, and A. Mecozzi, "The Ergodic GN Model for Space-Division Multiplexing With Strong Mode Coupling", *J. Lightw. Technol.*, vol. 40, no. 10, pp. 3263–3276, 2022. DOI: 10.1109/JLT.2022.3160207.
- [15] T. Hayashi, "Multi-core Fibers for Space Division Multiplexing", in *Handbook of Optical Fibers*, Singapore: Springer, 2019. DOI: 10.1007/978-981-10-1477-2\_66-1.
- [16] R. Dar, M. Feder, A. Mecozzi, and M. Shtaif, "Accumulation of nonlinear interference noise in multi-span fiber-optic systems", *Opt. Express*, vol. 22, no. 12, pp. 14199–14211, Jun. 2014. DOI: 10.1364/OE.22.014199.
- [17] C. Lasagni, P. Serena, A. Bononi, A. Mecozzi, and C. Antonelli, "Dependence of nonlinear interference on mode dispersion and modulation format in strongly-coupled SDM transmissions", *Opt. Express*, (early access), 2023. DOI: 10.1364/OE.484302.